PREDICTING TENSILE BEHAVIOUR OF HYBRID CARBON FIBRE/SRPP COMPOSITES: HOW FAR CAN ANALYTICAL MODELS TAKE US?

M. Selezneva[1], Y. Swolfs[1], A. Katalagarianakis[1], N. Hirano[2], I. Taketa[3], T. Karaki[2], I. Verpoest[1], L. Gorbatikh[1]

[1]Department of Materials Engineering, KU Leuven, Kasteelpark Arenberg 44, 3001 Leuven, Belgium
[2]Composite Materials Research Laboratories, Toray Industries, Inc., 1515 Tsutsui Masaki-cho Iyogun, 791-3193 Ehime, Japan
[3]Technical Center, Toray Carbon Fibers Europe S.A. (CFE), Route Départementale 817, 64170 LACQ, France

Keywords: pseudo-ductility, hybrids, self-reinforced composites, thermoplastics

Abstract
Hybrid composites combining brittle and ductile reinforcing fibres can achieve a superior combination of stiffness and toughness in comparison to the conventional single fibre type composite materials. The recently developed carbon fibre/self-reinforced polypropylene hybrids have demonstrated a unique combination of stiffness and toughness. Further optimisation of these hybrids can be achieved through modelling. This paper explores the capabilities and limitations of an analytical modelling technique. It was found that the sequence of the failure events, which depend on the critical stresses, and the overall shape of the stress-strain curve can be predicted analytically. Further work is required to accurately predict the critical strain values, which are needed for the estimation of the ultimate failure strain.

1. Introduction

Pseudo-ductile hybrid composites have gained a lot of interest over the past decade. Self-reinforced polypropylene (SRPP) composites hybridised with carbon-fibres can achieve 2x higher stiffness and 4x higher yield stress than SRPP while maintaining a high failure strain of over 6% [1]. Development of analytical tools would facilitate the optimisation of these hybrids for a given application and provide greater design flexibility. Jalalvand et al. [2] have developed a modelling strategy to analyse the tensile behaviour of pseudo-ductile hybrids with linearly elastic sub-laminates (e.g. carbon or glass fibre plies). The stress-strain curves are constructed by defining critical points associated with possible failure events, such as fragmentation of the brittle or low elongation layer, delamination and the final failure of the ductile or high elongation layer, as shown in Fig. 1. However, this modelling approach is yet to be applied to hybrids with more complex architectures and non-linear material behaviour. This paper explores the applicability of this analytical framework to carbon fibre/SRPP hybrids.

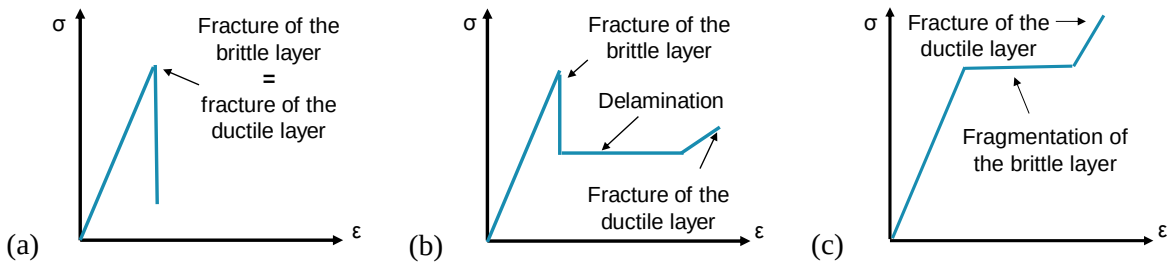

Figure 1. Stress-strain curves corresponding to the different failure events after the fracture of the brittle layer: a) failure of the ductile layer, b) delamination and c) stable fragmentation [2].

2. Materials and manufacturing

Hybrid panels were prepared from layers of twill 2/2 PP tape fabric (Propex Fabrics GmbH), dry mats with 6 mm long carbon fibres and an areal weight of 30 g/m^2 (Toray Industries, Inc.), and 20 µm thick maleic anhydride grafted polypropylene (MAPP) films (supplied by Toray Industries, Inc.). MAPP films were used to impregnate the carbon mats. All hybrids had SRPP as the outer layer (one ply on each side) and the carbon layer as the inner part. During the layup, dry carbon mats were interleaved with MAPP films to achieve good impregnation. Different overall carbon fibre volume fractions (V_f = 4.4 – 12.3 %) were achieved by varying the number of carbon mats (and MAPP films). The same internal fibre volume fractions of 16.7 % (four MAPP films per one 30 g/m^2 mat) in the impregnated carbon layer was maintained. Carbon/MAPP and SRPP panels were produced as reference materials. Panels were manufactured by hot compaction at 188°C with a hold time of 5 min at 40 bar, and an average cooling rate of 35°/min. Additional information on the manufacturing process can be found in [3].

Cut-ply specimens were used to investigate the onset of delamination growth from an existing crack and to measure fracture toughness as was done in [4, 5]. The panels were produced in 3 steps. First, a carbon/MAPP panel with V_f = 16.7 % was preconsolidated. Next, it was cut in half to create a slit and taped along the cut edges to induce a pre-crack representing an initial delamination. Finally, these layers were consolidated with one layer of twill PP tape fabric on each side. No additional films were added. The final V_f was 9.8 %.

3. Tensile tests

To measure the tensile properties of the pristine and the cut-ply hybrids, the ASTM D3039 standard was followed. Specimens were 250 mm long and 25 mm wide, and had a gauge length of 150 mm. Specimens were not tabbed, but instead a piece of emery cloth was placed between the specimen and the grips to prevent slippage. SRPP and hybrid specimens were loaded at a rate of 7.5 mm/min (5%/min), and carbon fibre/PP specimens at 2 mm/min (1.3%/min). The speed was adjusted to comply with the recommendations for the test duration given in the ASTM standard. Strain was measured using the 2D digital image correlation (DIC) technique and data was analysed using the VIC-2D software.

4. Analytical modeling

4.1. Behaviour up to the failure of the low elongation layer

The initial modulus of the hybrid before any damage occurs in the low elongation layer can be estimated using the rule-of-mixtures. To account for the non-linear behaviour of SRPP, stress-strain curve of a hybrid can be calculated by applying the rule-of-mixtures at incremental values of strain (ε_i), as shown in Eq. 1.

$$\sigma_i = \frac{(\sigma_H)_i \cdot t_H + (\sigma_L)_i \cdot t_L}{t_H + t_L}, \quad (1)$$

where σ_H and σ_L are stresses in the high elongation layer (SRPP) and low elongation layer (carbon/MAPP) at strain ε_i, σ_i is global stress in the hybrid at strain ε_i, and t_H and t_L are the half of the total thickness of the high and low elongation materials in the hybrid. To calculate the stress in the hybrid (σ_{LF}) at the time of the carbon ply failure, strength of the carbon ply (S_L) is substituted into Eq. 1 instead of σ_L, as is shown in Eq. 2. It is assumed that the carbon layer in the hybrid fails at the same strain (about 2 %) as the carbon/MAPP composite on its own. Hence, in Eq. 2 the stress in SRPP at 2 % strain is used at ($\sigma_{H(\varepsilon=2\%)}$).

$$\sigma_{LF} = \frac{\sigma_{H(\varepsilon=2\%)} t_H + S_L t_L}{t_H + t_L} \quad (2)$$

4.2. Failure of the high elongation layer

The maximum stress that can be sustained by the hybrid (σ_{HF}) following the fracture of the carbon fibre layer is estimated by setting the stress carried by the carbon layer in the cracked region to zero ($\sigma_L = 0$) and by substituting the strength of SRPP (S_H) instead of σ_H into Eq. 1, as shown in Eq. 3.

$$\sigma_{HF} = \frac{S_H t_H}{t_H + t_L} \tag{3}$$

When $\sigma_{HF} > \sigma_{LF}$, SRPP layers can sustain a higher stress than that at which the carbon fibre ply fracture initially occurred, and the hybrid continues to carry load until the maximum value (σ_{HF}). With this configuration, it is possible to achieve gradual fragmentation of the carbon layer. If $\sigma_{HF} < \sigma_{LF}$, SRPP plies alone cannot sustain a load higher than that at which the carbon fibre ply breaks, and there will be an immediate load drop. The ability of this strength-based criterion to predict the ultimate tensile strength of SRPP-based hybrids was shown in [1].

4.3. Delamination propagation

Expressions that relate fracture toughness to the stress or load required for delamination growth in UD glass or carbon fibre laminates can be found in [4, 5]. In the case of hybrids, similar equations were found in the field of fibre metal laminates [6-8] and carbon/glass hybrids [2]. In these papers, materials were treated as linearly elastic. In this section, the criterion based on fracture toughness will be derived to predict the load drop due to delamination in hybrids composed of materials with non-linear behaviour. The overall approach is similar to that observed in the aforementioned publications, but non-linear materials properties are considered. Fig. 2 depicts the geometry of a delaminating hybrid. Delamination propagation is considered to be uniform along all the interfaces, and hence a quarter of the geometry is considered. Subscripts *1* and *2* represent the delaminated and intact sections.

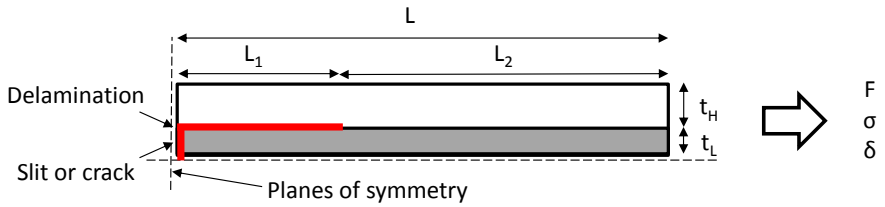

Figure 2. Schematic of a hybrid with delamination

The energy release rate (G_{II}) for a crack area increment (dA_1) or length increment (dL_1) is given by:

$$G_{II} = -\frac{dU}{dA_1} = -\frac{dU}{w dL_1} \ , \tag{4}$$

Where U is the strain energy stored in the body, and w is the specimen width. It is noteworthy that Eq. 4 valid for non-linearly elastic materials under the constant displacement assumption. This is an acceptable assumption since the abrupt load drop during unstable delamination growth (Fig. 1b) occurs at constant displacement, and the carbon layer is expected to release the strain energy elastically when it debonds from SRPP. The behaviour of SRPP in the intact region is also assumed to be elastic at low strains (< 2%). The total strain energy stored in the system can be computed from the applied force F and the displacement δ by considering the deformation of the delaminated ($d\delta_1$) and bonded ($d\delta_2$) sections separately.

$$U = \int_0^{\delta} F d\delta \ = \ \int_0^{\delta_1} F d\delta_1 + \int_0^{\delta_2} F d\delta_2 \tag{5}$$

Force is related to stress via $F = wt\sigma$. To account for the non-linear behaviour of the SRPP in section (1) and the intact hybrid in section (2), material properties were estimated using a power-law:

$$\sigma = C\varepsilon^N,$$

Where the coefficient C represents stiffness of the material if $N = 1$. The power law expression for the intact hybrid up to σ_{LF} can be estimated by fitting the stress-strain curve obtained using Eq. 1, alternatively it can be treated as a linear material by setting $N = 1$. Next, the relations for force, stress and strain are substituted into Eq. 5 to express the strain energy in terms of strain.

$$U = w\int_0^{\delta_1} C_1\varepsilon_1^{N_1} t_H d\delta_1 + w\int_0^{\delta_2} C_2\varepsilon_2^{N_2}(t_H + t_L)d\delta_2$$

By expressing strain in terms of displacement and length in the above equation and integrating it, the following equation for the strain energy in the hybrid is obtained,

$$U = w\frac{C_1 t_H}{N_1+1}{\delta_1}^{N_1+1}{L_1}^{-N_1} + w\frac{C_2(t_H+t_L)}{N_2+1}{\delta_2}^{N_2+1}(L-L_1)^{-N_2} \quad (6)$$

Next, Eq. 6 is substituted into Eq. 4 and differentiated with respect to the delamination length (L_1).

$$G_{II} = \frac{N_1}{N_1+1}C_1 t_H(\varepsilon_1)^{N_1+1} - \frac{N_2}{N_2+1}C_2(t_H+t_L)(\varepsilon_2)^{N_2+1}$$

To simplify the above equation, strain can be converted back into stress via $\sigma = C\varepsilon^N$. The global stresses are related to the local stresses in the following manner:

$$\sigma = \sigma_2 = \sigma_1\left(\frac{t_H}{t_H+t_L}\right).$$

Delamination development is predicted when the interlaminar energy release rate becomes equal to or higher than the critical energy release rate ($G_{II} = G_{IIc}$) [2]. The critical stress that is needed for the crack to propagate is hence set to $\sigma = \sigma_{del}$. The resultant expression relating fracture toughness to the stress at delamination is given below.

$$G_{IIc} = \frac{N_1}{N_1+1}\frac{t_H}{C_1^{\frac{1}{N_1}}}\left(\frac{\sigma_{del}(t_H+t_L)}{t_H}\right)^{1+\frac{1}{N_1}} - \frac{N_2}{N_2+1}\frac{(t_H+t_L)}{C_2^{\frac{1}{N_2}}}(\sigma_{del})^{1+\frac{1}{N_2}} \quad (7)$$

In this expression the subscript *1*, which represents the delaminated section, can be replaced by the subscript *H*, which represents properties of the high elongation material. By setting $N = 1$, the equation for linearly elastic materials is obtained and coincides with the one in [2]:

$$G_{IIc} = \frac{(\sigma_{del})^2(t_L+t_H)^2}{2}\left(\frac{1}{C_H t_H} - \frac{1}{C_H t_H + C_L t_L}\right), \quad (8)$$

or rearranged for stress [2]:

$$\sigma_{del} = \frac{1}{(t_L+t_H)}\sqrt{\left(2G_{IIc}\frac{(C_H t_H)(C_H t_H + C_L t_L)}{C_L t_L}\right)}. \quad (9)$$

According to Eq. 9 during stable crack growth, the applied stress is independent of delamination length and stays constant. If applied stress is lower than the delamination stress ($\sigma_{LF} < \sigma_{del}$), no crack is expected. If the applied load becomes equal to or greater than the delamination stress ($\sigma_{LF} \geq \sigma_{del}$), the crack starts to propagate until the stress level reduces to below σ_{del} [2].

4.4. Fragmentation

Gradual fragmentation of the carbon layer is assumed to occur at the constant stress level (σ_{LF}). This is based on the assumption of the constant strength of the carbon layer. To calculate the strain at the end of the fragmentation process, Jalalvand et al. [2] used the Kelly-Tyson approach to calculate the stress distribution in the low elongation material and the statistical variation of the length between the ply fractures or cracks. Jalalvand el al. [2] showed that the average post-fragmentation stress in the low elongation material ($\sigma_{L@pfrag}$) is only a function of the failure strength S_L, as shown in Eq. 10.

$$\sigma_{L@pfrag} = \frac{7}{18} S_L. \tag{10}$$

For linearly elastic materials, the modulus of the hybrid (E_{frag}) with randomly saturated fragmentation is given by [2]:

$$\frac{1}{E_{frag}} = \frac{1}{E_H}\left(1 + \beta - \frac{7}{18}\frac{\alpha\beta(1+\beta)}{(1+\alpha\beta)}\right),$$

where α and β are the ratios of modulus and thickness: $\alpha = E_L/E_H$ and $\beta = t_L/t_H$. Strain at the end of fragmentation is computed via $\varepsilon_{frag} = \sigma_{LF}/E_{frag}$. The post-fragmentation behaviour (pfrag) of the hybrid is given by [2]:

$$\sigma_{@pfrag} = \frac{E_H}{1+\beta}\varepsilon_{@pfrag} + \frac{7}{18} S_L \frac{\beta}{1+\beta}$$

This equation becomes valid from $\sigma_{@pfrag} = \sigma_{LF}$. To account for the non-linearity of the SRPP, the left-hand of the equation is modified analogous to Eq. 1.

$$\left(\sigma_{@pfrag}\right)_i = \frac{(\sigma_H)_i}{1+\beta} + \frac{7}{18} S_L \frac{\beta}{1+\beta} \tag{11}$$

5. Results and discussion

5.1. Cut-ply specimens

The stress-displacement curves of the pristine (i.e. not cut) and the cut-ply specimens with the same V_f are presented in Fig. 3. It was found to be difficult to unambiguously identify the onset of tape debonding, because individual tapes began to debond gradually (Fig. 3) and there was no uniform front. There were also no significant changes to the stress-strain curve or easily identifiable features, see red curve in Fig. 3, which could be linked to debonding or delamination. For instance, in the work of Jalalvand et al. [2] stable delamination propagation corresponded to a stress plateau. In the case of SRPP hybrids, the upper stress level, which resembles a plateau (σ_{HF}), was related to the failure stress of SRPP.

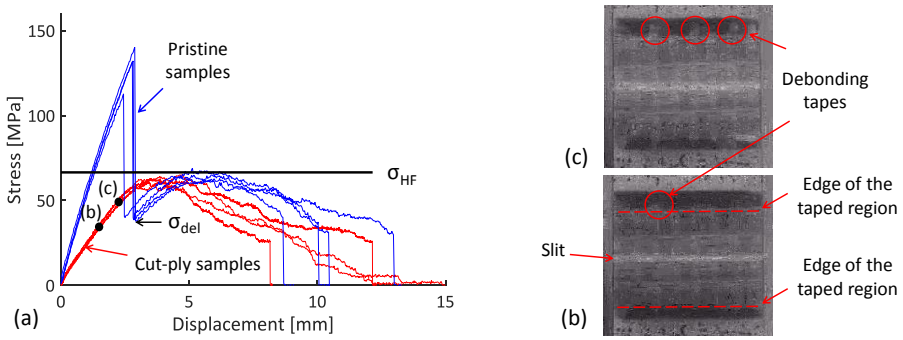

Figure 3. Behaviour of hybrids during debonding of the SRPP layers: (a) comparison of the stress-displacement curves of the cut-ply and pristine samples, and (b) and (c) debonding patterns observed on the cut-ply specimens.

To avoid the ambiguity, the critical stress for delamination (σ_{del}) was extracted from the curves of the pristine samples, see blue curve in Fig. 3. This method is based on the assumption that the stress drop occurs entirely due to the unstable delamination growth, rather than any damage sustained by the SRPP. Hence, this is an indirect measurement of σ_{del} and serves as an approximation technique for G_{IIc}. The main advantage of this method is that it allows for simple, consistent and unambiguous extraction of the σ_{del}. For this hybrid, G_{IIc} was calculated using Eq. 7 to be 600 J/mm². The following input parameters were used: C_1=0.491 GPa, N_1=0.72, t_H=0.142 mm, C_2=5.98 GPa, N_2=0.94, t_L=0.193 mm, σ_{del}=42 MPa.

5.2. Behaviour up to the failure of the low elongation layer

Comparison between the experimental and the modelling results of the stress-strain curves up to the failure of the carbon layer is presented in Fig. 4. Overall, a good correlation between the calculated and the measured data is observed. Additional results were published in [1].

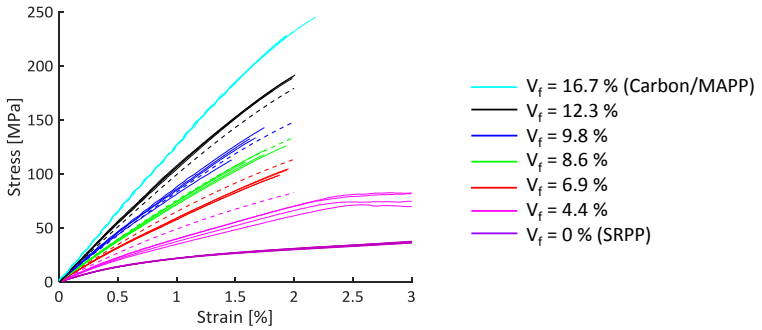

Figure 4. Experimental (solid lines) and modelling (dashed lines) results of the initial elastic portion of the stress-strain curves.

5.3. Failure of the high elongation layer

Two types of failure events are considered here: with and without a load drop. In Fig. 5a, a pseudo-ductile response is shown, and it is obtained when $\sigma_{HF} > \sigma_{LF}$. In Fig. 5b-e, hybrids experience a load drop after the initial failure of the carbon layer, but continue to carry load during stable delamination growth. The maximum load (σ_{HF}) reached in this regime can be estimated using the strength of SRPP (155 MPa). Additional results can be found in [1]. Tang et al. [9] showed that SRPP is damaged during the load drop (following failure of the carbon layer) and hence is expected to fail at an earlier load. Nonetheless, the proposed criterion provides a good estimate of the expected material behaviour.

5.4. Delamination

The critical stress that is required for delamination growth to occur was calculated using Eq. 7 and G_{IIc} = 600 J/mm². The input parameters for all the hybrids are given in Fig. 5. If the stress at which the carbon layer breaks is lower than the stress needed to drive the delamination growth ($\sigma_{LF} < \sigma_{del}$), no drop in the stress-strain curve is expected to occur, as shown in Fig. 5a. However, if $\sigma_{LF} > \sigma_{del}$, a load drop is expected to occur, as shown in Fig. 5b-e. Unsteady delamination growth occurs during this load drop. Once the load drops to the level of σ_{del}, further extension of the material is required to drive the delamination further. More energy/work must be added to the system for delamination to propagate. In the case of carbon/glass hybrids [2], stable delamination growth would occur at the constant stress level, in the case of SRPP-hybrids stress has to increase to drive delamination. Similar trends were observed in other works on SRPP hybrids [9, 10]. This behaviour can in part be attribute to the non-linear behaviour of SRPP.

The good correlation between the calculated and measured critical stress for delamination is observed in Fig. 5. This illustrates the usefulness of the proposed method and its potential as a design tool, even

though G_{IIc} was measured indirectly. It is a simple and powerful technique that can be used for conceptual design and allows for the estimation of the key points on the stress-strain curves and the sequence of failure events.

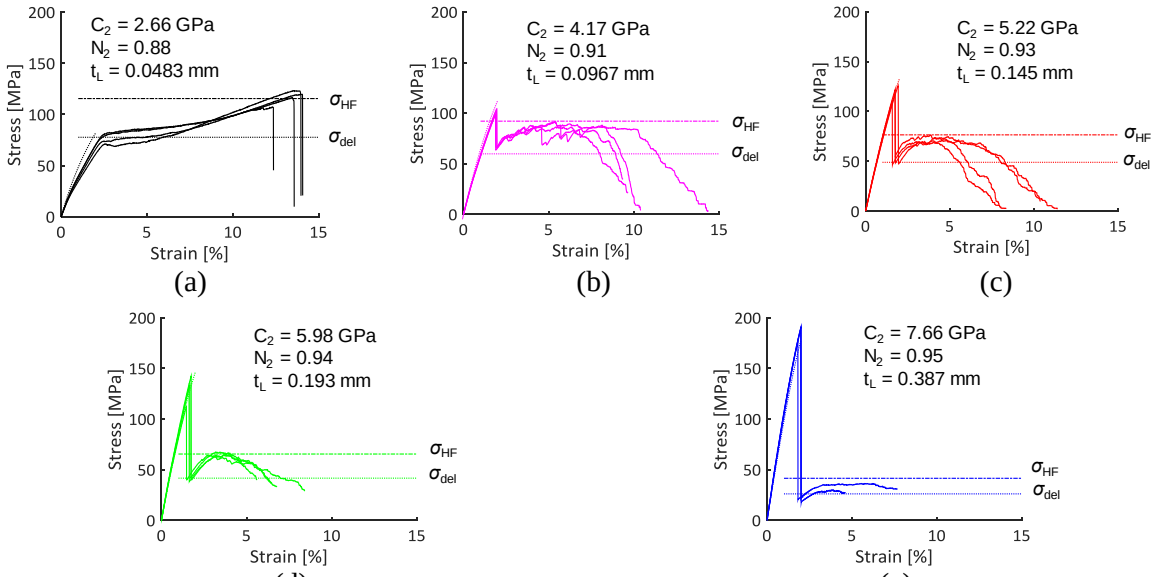

Figure 5. Stress-strain curves for hybrids with V_f of (a) 4.4%, (b) 6.9%, (c) 8.6%, (d) 9.8% and (e) 12.3%. The two horizontal lines represent the calculated σ_{HF} and σ_{del} stress level. Input parameters for SRPP are the same for all hybrids: C_H=C_1= 0.491 GPa, N_H=N_1=0.72, t_H=0.142 mm.

5.5. Fragmentation

Pseudo-ductile specimens developed white lines on the surface that correspond to the sites of the carbon-layer fragmentation, as shown in Fig. 6a. These observations suggested that the equations used to describe the fragmentation saturation in unidirectional carbon/glass hybrids might be applicable to these hybrids as well. Fig. 6b shows the estimated post-saturation section of the stress strain-curve of a pseudo-ductile hybrid. Fragmentation is assumed to occur at a constant stress level. Fragmentation saturation strain of the hybrid occurs at the point when $\sigma_{@pfrag} = \sigma_{LF}$. It is obvious that the saturation strain is over predicted, hence implying that the contribution or the stress retention of the damaged carbon layer is under predicted. Hence, another tool is needed to capture the gradual damage development of the carbon layer (randomly-oriented discontinuous fibres) in SRPP-based hybrids.

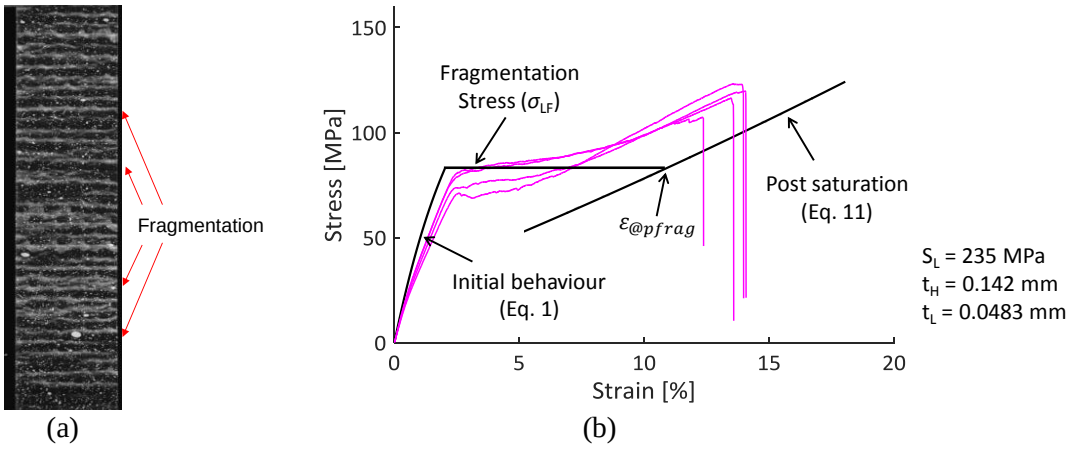

Figure 6. Pseudo-ductile hybrid with V_f 4.4 %: a) fragmentation observed on the surface and b) stress-strain behaviour of the hybrid.

5.6. Failure strain

Estimation of the ultimate failure strain ($\varepsilon_{failure}$) is difficult as it depends on the sequence of the failure events [2]. Failure strain of fully brittle hybrids is assumed to occur at the failure strain of carbon/MAPP layer and is estimated to be 2%. In the event of the complete delamination, as shown in Fig. 1b, $\varepsilon_{failure}$ corresponds to the failure strain of the high elongation material. However, in the case of carbon/SRPP hybrids delamination does not span the whole length of the hybrids, and their $\varepsilon_{failure}$ is lower than the failure strain of SRPP (20%), see Fig. 5b-e. Failure strain of the pseudo-ductile hybrids cannot be calculated either, because stress retention of the fragmented/damaged carbon layer cannot be predicted accurately thus far.

6. Conclusions

The analytical modelling approach that was developed for unidirectional carbon/glass hybrids [2], was extended to include the non-linearity of the constituents and applied to carbon/SRPP hybrids to predict the sequence of the failure events. The main issue remains the calculation of the stress retention of the damaged or fragmented carbon layer, which is needed for the prediction of the failure strain of the pseudo-ductile hybrid.

Acknowledgments

The authors would also like to acknowledge the funding and the materials provided by Toray Industries. Yentl Swolfs also extends his gratitude to the FWO Flanders for his postdoctoral fellowship.

References

1. Selezneva, M., et al., The brittle-to-ductile transition in tensile and impact behavior of hybrid carbon fibre/self-reinforced polypropylene composites. Composites Part A, 109:20-30, 2018.
2. Jalalvand, M., G. Czél, and M.R. Wisnom, Damage analysis of pseudo-ductile thin-ply UD hybrid composites - a new analytical method. *Composites Part A*, 69:83-93, 2015.
3. Swolfs, Y., et al., The influence of weave architecture on the mechanical properties of self-reinforced polypropylene. *Composites Part A*, 53:129-136, 2013.
4. Cui, W.C., M.R. Wisnom, and M. Jones, An experimental and analytical study of delamination of unidirectional specimens with cut cetral plies. *Journal of Reinforced Plastics and Composites*, 13(8):722-739, 1994.
5. Daelemans, L., et al., Improved fatigue delamination behaviour of composite laminates with electrospun thermoplastic nanofibrous interleaves using the Central Cut-Ply method. *Composites: Part A*, 94:10–20, 2017.
6. Lin, C.T. and P.W. Kao, Fatigue delamination fibre-reinforced growth in carbon aluminium laminates. *Composites Part A*, 27A: 9- 15, 1996.
7. Roderick, G., R. Everett, and J. Crews, Debond propagation in composite reinforced metals, in *Fatigue of Composite Materials, STP569*. American Society for Testing of Materials, 295-306, 1975.
8. Alderliesten, R.C., J. Schijve, and S.v.d. Zwaag, Application of the energy release rate approach for delamination growth in Glare. *Engineering Fracture Mechanics*,73:697–709, 2006.
9. Tang, J., et al., Discontinuities as a way to influence the failure mechanisms and tensile performance of hybrid carbon fiber/self-reinforced polypropylene composites. *Composites Part A*, 107:354-365, 2018.
10. Swolfs, Y., et al., Introducing ductility in hybrid carbon fibre/self-reinforced composites through control of the damage mechanisms. *Composite Structures*, 131:259-265, 2015.